

Laser co-photolytic approach to copper(I) bromide/ polymer nanosol and nanocomposite

Josef Pola^{a,*}, Akihiko Ouchi^{b,**}, Petr Bezdička^c, Jaroslav Boháček^c, Jan Šubrt^c

^a Institute of Chemical Process Fundamentals, Academy of Sciences of the Czech Republic, 16502 Prague, Czech Republic

^b National Institute of Advanced Industrial Science and Technology, AIST, Tsukuba, Ibaraki 305-8565, Japan

^c Institute of Inorganic Chemistry, Academy of Sciences of the Czech Republic, 25068 Řež, Czech Republic

Received 29 January 2007; received in revised form 6 March 2007; accepted 8 March 2007

Available online 12 March 2007

Abstract

KrF laser co-photolysis of Cu(II) acetylacetonate and 1-bromoeicosane in 2-propanol results in the formation of CuBr/polymer colloidal solution aging of which results in sedimentation of CuBr/polymer nanocomposite. This clean process involves a reaction between two photo-products (nano-sized Cu and a brominating reagent) and photolytic formation of polymer. The CuBr nanoparticles embedded in a photo-produced polymer possess zinc blende-type cubic structure. The co-photolytic procedure represents a new approach to polymer-stabilized nano-inorganic compounds. © 2007 Elsevier B.V. All rights reserved.

Keywords: Co-photolysis; CuBr/polymer nanosol; Cu/Br/polymer nanocomposite

1. Introduction

Copper(I) bromide nanoparticles in dielectric media have received much recent attention with respect to quantum-size effects, interesting luminescence properties and their applications as optical filters.

The CuBr nanoparticles dispersed in glasses were prepared by dissolving CuBr in the course of silicate glass formation [1], copper staining of Br⁻ ion-containing glass [2], Cu + Br ion implantation of silica glass and subsequent heating to 1100 °C [3], and by incorporation of CuBr during the sol-gel process [4–6]. The nanoparticles in polymers were obtained by dissolving CuBr and polymer in organic solvent and subsequent heat-induced solvent removal [7,8]. Another approach to CuBr/polymer nanocomposites can be sol-gel/emulsion technique-assisted reaction between CuO and KBr [9,10].

We have recently shown that simultaneous laser-induced decomposition of two different volatile (organometallic and heterorganic) compounds in the gas phase results in generation of two different elements in the gas phase and allows reaction

between them leading to the formation of nano-sized inorganic compounds (SnS and SnS₂ [11], GeS, GeS₂ [12] and SnTe [13]). These nano-inorganic compounds are feasibly formed due to small size of the reacting species and negative heats of product formation and they become protected by polymer that is simultaneously produced from the organic portion of the educts. Such method is restricted to volatile compounds and up to now, no such approach to nano-inorganic compounds using laser co-photolysis of two different educts has been described for the liquid phase.

In this paper, we report on KrF laser co-photolysis of Cu(II) acetylacetonate and bromoalkane (1-bromoeicosane) in 2-propanol and show that this co-photolysis yields colloidal solutions of photo-polymer-coated CuBr nanoparticles, which produce a sediment of CuBr/polymer nanocomposite upon aging. The co-photolysis, thus, represents a novel approach to CuBr nanoparticles in dielectric matrix and is the first example of the co-photolytic formation of nano-inorganic compound in the liquid phase.

2. Experimental

1-Bromoeicosane (TCI, 2×10^{-4} mol) was added to 50 ml of 1.5×10^{-3} M solution of Cu(II) acetylacetonate (Aldrich) in 2-propanol (Cica-reagent for spectroscopy) in a quartz tube

* Corresponding author. Tel.: +420 2 20390308; fax: +420 2 20920661.

** Corresponding author. Tel.: +8129 861 4550; fax: +8129 861 4421.

E-mail addresses: pola@icpf.cas.cz (J. Pola), ouchi.akihiko@aist.go.jp (A. Ouchi).

(3 cm in diameter, 10 cm long) equipped with a valve for connection to a vacuum line. The solution was de-aerated by using vacuum (three freeze–thaw cycles), bubbled with Ar and irradiated with an LPX-200 (Lambda Physik) laser at 248 nm for 1 h at a repetition frequency of 10 Hz and energy of 650 mJ per pulse (measured by a Gentec ED-500 joulemeter). The solution was stirred by a magnetic bar and the laser pulses were mildly focused to incident area of 1.2 cm² to obtain incident fluence of 540 mJ/cm². Temperature of the solution during the irradiation has increased in few minutes to less than 50 °C and stayed at this value.

The photolytic progress was monitored on the aliquots (0.5 ml) withdrawn from the irradiated solution and diluted with hexane (Cica-reagent for spectroscopy, 3 ml) by UV–vis spectrometry (a Shimadzu UV-2450 UV–vis spectrometer) in the 4 ml quartz cells. After the irradiation, the solution was left overnight and yielded black sediment that was centrifuged, washed with hexane, again centrifuged and kept under argon.

The irradiated solution was analyzed on a Shimadzu QP5050 gas chromatograph-mass spectrometer (60 m long capillary column with Neutrabond-1 as a stationary phase, programmed temperature 30–200 °C) and the detected photolytic products were identified by using the NIST library.

The sediment was analyzed by UV spectroscopy (a UV 1601 Shimadzu Spectrofotometer), FTIR spectroscopy (a Nicolet Impact Spectrometer), X-ray diffraction measurements and by electron microscopy. SEM images were acquired using a Philips XL30 CP scanning electron microscope. TEM analysis (particle size and phase analysis) was carried out on a Philips 201 transmission electron microscope. XRD diffraction database [14] and process diffraction [15] were employed to assign measured diffraction patterns.

A suspension of a powder in ethanol was placed on a Si zero-background sample holder. Diffraction patterns were collected with a PANalytical X'Pert PRO diffractometer equipped with a conventional X-ray tube (Co K α radiation, 40 kV, 30 mA) and a multichannel detector X'Celerator with an anti-scatter shield. X-ray patterns were measured in the range of 10–100° 2 θ with the step of 0.0167° and 80 s counting per step. We used 0.5° divergence and 1° anti-scatter slits, 0.04 rad Soller slits and a primary beam mask of 15 mm.

Qualitative analysis was performed with HighScore software package (PANalytical, Netherlands, version 1.0d), Diffrac-Plus software package (Bruker AXS, Germany, version 8.0) and JCPDS PDF-2 database [16].

3. Results and discussion

UV absorption spectrum of Cu(II) acetylacetonate consists of bands at 280–310, 230–255 and 190–210 nm [17,18] and that of monobromoalkanes shows bands peaked at ca. 210 nm and tailing to longer wavelengths [19,20]. KrF laser photolysis of both compounds is possible due to absorption of the 248 nm radiation in the second band of Cu(II) acetylacetonate (a charge-transfer transition of the ligand-to-metal type [17,18]) and in the $n \rightarrow \sigma^*$ transition [19] band of 1-bromoeicosane. These photolyses result in the homolysis of the C–Br bond [19,20] and in

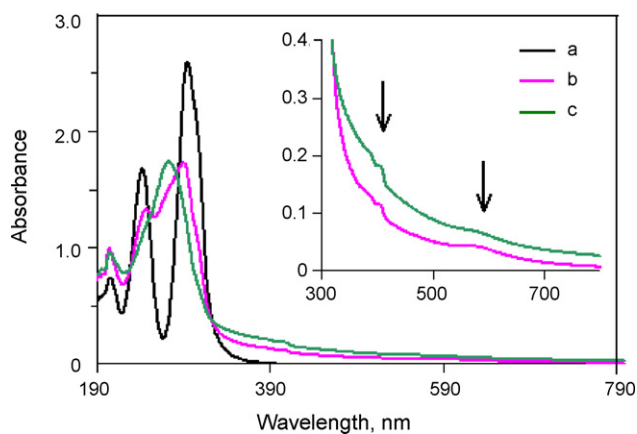


Fig. 1. Absorption spectra of Cu(II) acetylacetonate-1-bromoeicosane in 2-propanol (diluted in hexane) before (a), after 30 min (b) and 60 min (c) (irradiation with KrF laser). Weak bands at 385, 403 (CuBr nanosols) and 575 nm (Cu nanosols) are designated by arrows in an enlarged 300–790 nm region (inset).

the formation of Cu nanosols [21,22]. The molar absorptivity of Cu(II) acetylacetonate at 248 nm ($1.5 \times 10^4 \text{ dm}^3 \text{ mol}^{-1} \text{ cm}^{-1}$) is by ca. 4 orders of magnitude higher than that of monobromoalkanes [19]. This difference is compensated by the photochemical quantum yield of Cu(II) acetylacetonate depletion being by almost four orders of magnitude lower than that of the C–Br homolysis [19].

The KrF laser irradiation of the Cu(II) acetylacetonate-1-bromoeicosane solution results in pronounced darkening and UV–vis spectral changes of the irradiated solution. We observed depletion of absorption bands of the chelate and a build-up of a medium band at 270 nm (Cu aggregates [21–23]) and weak bands at 385, 403 (CuBr nanosols [6,7]) and 575 nm Cu nanosols (e.g. [24,25]) (Fig. 1).

Organic compounds—ethane, propene, acetaldehyde, acetone, 2,4-acetylacetonate and carboxylic acid esters (e.g. ethenyl acetate, 2-propenyl acetate, 1-methylethyl acetate and ethyl 2-oxo-propanoate) detected by GC/MS analysis are in keeping with a number of photolytic decomposition steps including photolysis of both photo-produced [26] acetylacetonate and 2-

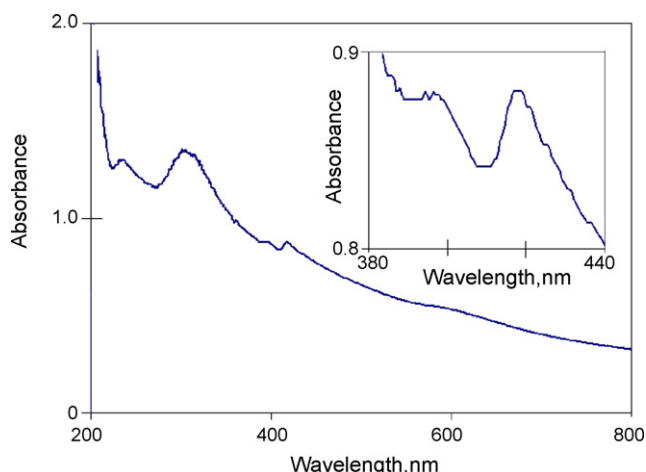


Fig. 2. UV–vis spectrum of the sediment dispersed in 2-propanol.

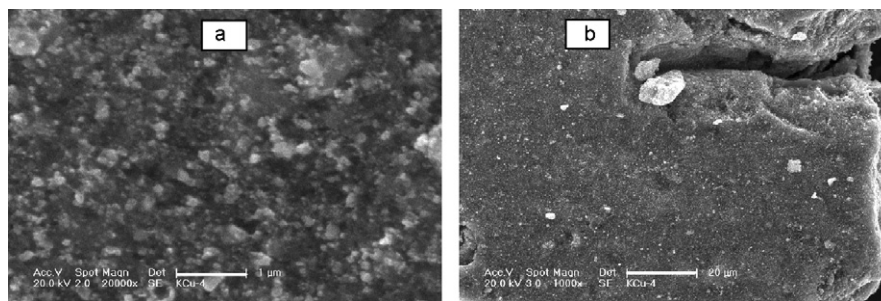


Fig. 3. SEM image of the sediment. Bar 1 μm (a) and 20 μm (b).

propanol and reactions of photo-fragments with 2-propanol and/or propene leading to a high-molecular substances [22]. The black solution is stable for almost whole day and then it undergoes sedimentation of ultrafine black particles and becomes transparent.

The UV–vis spectrum of the sediment washed with hexane and ultrasonically dispersed in 2-propanol (Fig. 2) consists of bands peaked at 230, 300, 396 and 417 nm of which the latter two correspond to the known $Z_{1,2}$ and Z_3 transitions of CuBr nanoparticles [6,7]. The two shorter wavelength-bands relate to an organic polymer produced photolytically from the solvent and liberated acetylacetone [22]. The FTIR spectrum of the sediment shows infrared bands at 679, 782, 810, 846, 1070, 1260, 1615, 3402 and 3508 cm^{-1} and is, indeed, compatible with an unsaturated polymer containing C=C, C–H, C–O and O–H bonds. The UV–vis absorption pattern (Fig. 2) is consistent with some degree of conjugation of the C=C bonds.

The SEM analysis of the sediment reveals large agglomerates composed of bodies smaller than $0.5\ \mu\text{m}$ (Fig. 3). The elemen-

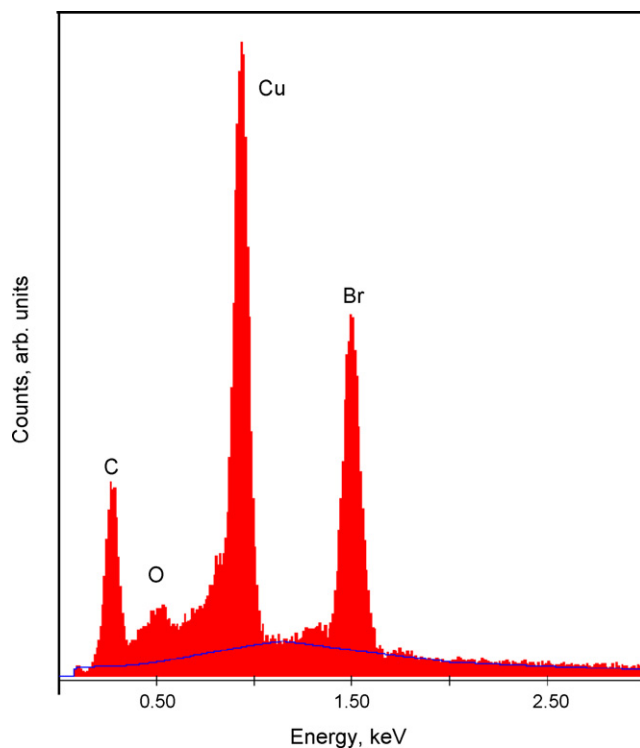


Fig. 4. EDX–SEM analysis of the sediment.

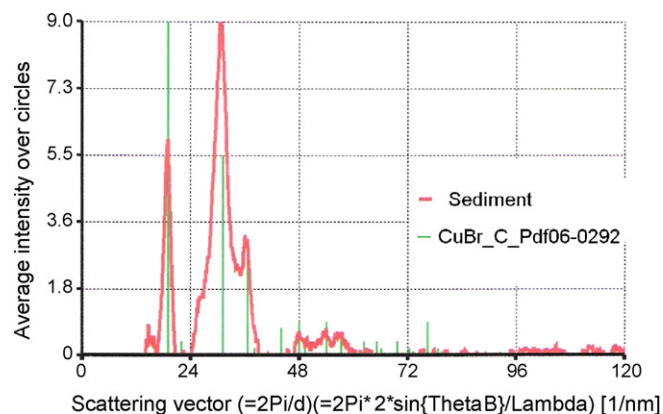


Fig. 5. Electron diffraction pattern of the sediment.

tal composition of the sediment determined by the EDX–SEM analysis (Fig. 4) – $\text{Cu}_{1.00}\text{Br}_{0.92}\text{C}_{2.20}\text{O}_{0.03}$ – reveals comparable amounts of Cu and Br elements, the substantial amount of C and a low amount of O elements.

Electron diffraction analysis (Fig. 5) and X-ray diffraction analysis (Fig. 6) of the sediment reveal the cubic pattern of crystalline γ -CuBr (face centered cubic, PDF 6-292).

HREM images of the sediments (Fig. 7) show agglomerated, several nm-sized bodies in which the crystalline phase is surrounded by an amorphous phase.

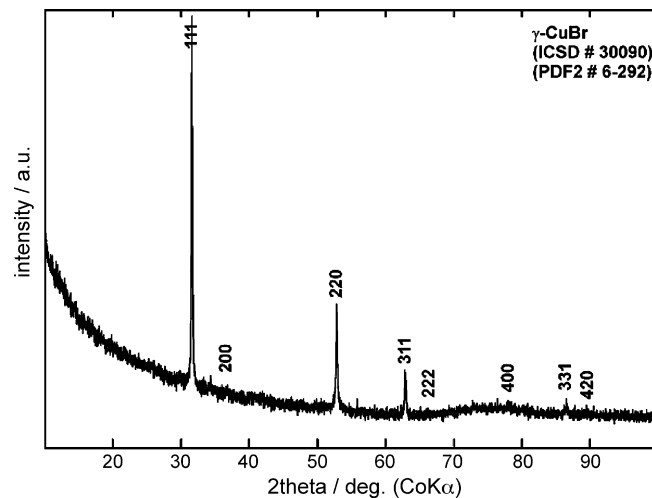


Fig. 6. X-ray diffraction pattern of the sediment.

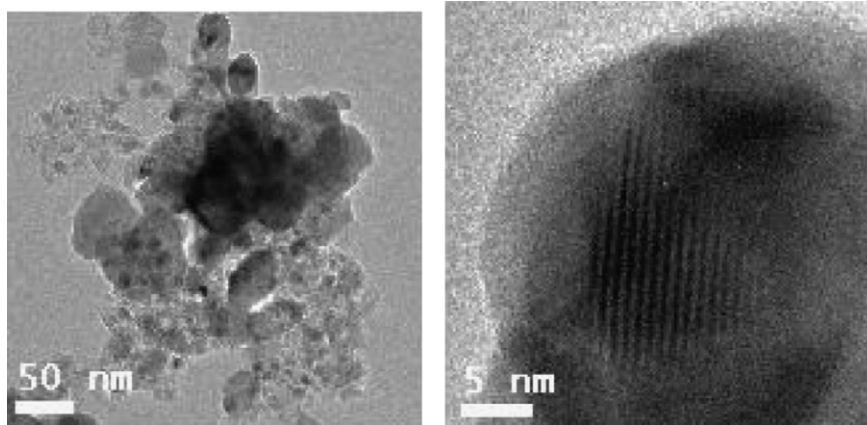


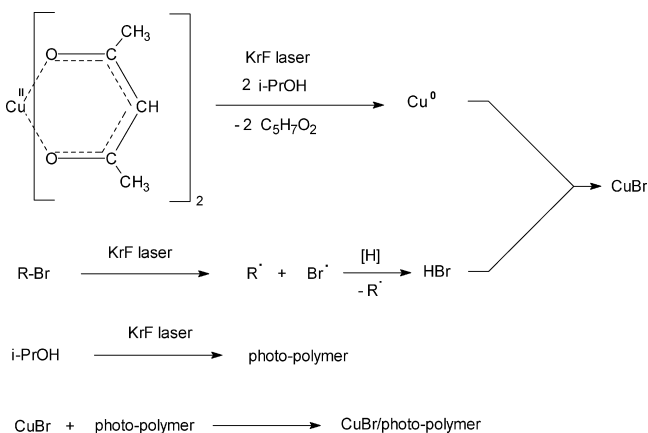
Fig. 7. HREM image of the sediment.

These analyses are, therefore, compatible with cubic nanoparticles of cuprous bromide covered with photo-polymeric layers.

The formation of CuBr can, in principle, occur by several routes. An independent observation of stability of Cu nanosols towards added 1-bromoeicosane in 2-propanol rules out the Br atom abstraction from bromoalkane by Cu clusters. Other feasible routes are Cu + Br, Cu + HBr and Cu + Br₂ steps. We note that the HBr and Br₂ formations have similar pre-exponential factors, but the Br atoms combination [27] has sizeable activation energy, whereas [H] abstraction by Br atom [28] has almost zero activation energy. We assume that the Cu + HBr route is more plausible than the Cu + Br or the Cu + Br₂ route [29], as the formation of the CuBr species requires the Br escape from the solvation shell that gives the opportunity to the [H] abstraction reaction. The most probable steps of the CuBr formation are, therefore, those envisaged in Scheme 1.

The ca. 10 nm size of CuBr indicated by HREM analysis (Fig. 7) is in line with efficient polymer stabilization of relatively small particles.

We note that the cuprous halides are known to crystallize at room temperature with zinc blende-type cubic structure (γ -CuBr) and upon heating they transform to hexagonal wurtzite-type structure (385 °C, β -CuBr) and further to cubic form (470 °C, α -CuBr) [30].



The CuBr nanoparticles embedded in the photo-polymer and obtained at temperature less than 50 °C possess zinc blende-type cubic structure (γ -CuBr). We note that the same “room temperature” crystalline form was also observed in the CuBr nanoparticles dispersed in the borosilicate glasses treated to 510 °C [2] and in the CuBr particles in silica glasses heated to 900 [4] and 1100 °C [3].

The reported co-photolytic technique involving bromination of Cu nanosols adds to little studied reactivity of Cu nanoparticles [31,32] and it is expected to be used for synthesis of other nano-inorganic compounds.

4. Conclusion

CuBr/polymer colloidal solution was obtained by KrF laser co-photolysis of Cu(II) acetylacetonate and 1-bromoeicosane in 2-propanol. This solution yielded fine CuBr/polymer nanocomposite particles as sediment upon 1 day aging. The CuBr nanoparticles embedded in a photo-produced polymer have zinc blende-type cubic structure. The reported co-photolysis represents a clean process involving reaction between two photo-products (Cu and a brominating reagent) and photo-polymerization and it represents a new approach to polymer-stabilized nano-inorganic compounds.

Acknowledgement

The authors are grateful to Dr. Bakardjieva for HREM analysis.

References

- [1] A.I. Ekimov, A.L. Efros, A.A. Onuschenko, *Solid State Commun.* 56 (1985) 921.
- [2] K. Kadono, T. Suetsugu, T. Ohtani, T. Einishi, T. Tarumi, T. Yazawa, *J. Mater. Res.* 20 (2005) 2480.
- [3] K. Fukumi, A. Chayahara, A. Kinimura, H. Kageyama, K. Kadono, N. Kitamura, J. Nishii, Y. Horino, *J. Mater. Res.* 18 (2003) 885.
- [4] M. Nogami, Y.Q. Zhu, K. Nagasaka, *J. Non-Cryst. Solids* 134 (1991) 71.
- [5] A. Kriltz, R. Facht, M. Müller, H. Bürger, *J. Sol-Gel Sci. Technol.* 11 (1998) 197.
- [6] G. Suyal, M. Mennig, H. Schmidt, *J. Mater. Chem.* 13 (2003) 1783.

- [7] H. Yao, T. Hayashi, Chem. Phys. Lett. 197 (1992) 21.
- [8] M. Oda, M.Y. Shen, T. Goto, Int. J. Mod. Phys. B 29–30 (2001) 3912.
- [9] M. Yang, J.J. Zhu, J.J. Li, J. Cryst. Growth 267 (2004) 283.
- [10] M. Yang, J.J. Zhu, Mater. Res. Bull. 40 (2005) 265.
- [11] R. Tomovska, V. Vorlíček, J. Boháček, J. Šubrt, J. Pola, New J. Chem. 29 (2005) 785.
- [12] R. Tomovska, V. Vorlíček, J. Boháček, J. Šubrt, J. Pola, J. Photochem. Photobiol. A: Chem. 182 (2006) 107.
- [13] D. Pokorná, J. Boháček, V. Vorlíček, J. Šubrt, Z. Bastl, E.A. Volnina, J. Pola, J. Anal. Appl. Pyrol. 75 (2006) 65.
- [14] DiffractPlus, version 8.0, Bruker AXS, 2002.
- [15] J.L. Lábár, in: L. Frank, F. Ciampor (Eds.), Proceedings of EUREM 12, Czechoslovak Society for Electron Microscopy, Brno, Czech Republic, 2000, p. 1379.
- [16] Powder Diffraction File, Release 2000. PDF-2, International Centre for Diffraction Data; Newton Square, PA, U.S.A.
- [17] J.P. Fackler, F.A. Cotton, W. Barnum, Inorg. Chem. 2 (1963) 97.
- [18] J.P. Fackler, F.A. Cotton, Inorg. Chem. 2 (1963) 102.
- [19] J.G. Calvert, J.N. Pitts, Photochemistry, J. Wiley, New York, 1966.
- [20] K.-H. Jung, H.S. Yoo, J.S. Hwang, J. Photochem. 23 (1983) 289, and refs. therein.
- [21] A. Ouchi, Z. Bastl, J. Boháček, J. Šubrt, J. Pola, Surf. Coat. Technol. 201 (2007) 4728.
- [22] J. Pola, A. Ouchi et al., submitted for publication.
- [23] L. Khatouri, M. Mostafavi, J. Amblard, J. Belloni, Chem. Phys. Lett. 191 (1992), 351 and 135.
- [24] K. Kimura, Bull. Chem. Soc. Jpn. 57 (1984) 1683.
- [25] I. Lisiecki, M.P. Pileni, J. Am. Chem. Soc. 115 (1993) 3887.
- [26] H.D. Gafney, R.L. Lintvedt, J. Am. Chem. Soc. 93 (1971) 1623.
- [27] J.K.K. Ip, G. Burns, J. Chem. Phys. 51 (1969) 3414.
- [28] S.W. Benson, Thermochemical Kinetics, Wiley, New York, 1976.
- [29] C.Y. Nakakura, R.I. Altman, Surf. Sci. 398 (1998) 281, and refs. therein.
- [30] Comprehensive Inorganic Chemistry, vol. 3, Pergamon Press, Oxford, 1973, p. 26.
- [31] A. Yanase, H. Komiyama, Surf. Sci. 248 (1991) 11.
- [32] Y. Champion, F. Bernard, N. Guigue-Millot, P. Perriat, Mater. Sci. Eng. A 360 (2003) 258.